Heavy quarkonium production in the Regge limit of quantum chromodynamics

V. A. Saleev[a]*, D. V. Vasin[a]†
[a] *Samara State University*
Samara 443011, Russia

Abstract

The main results of our recent papers [1] are presented in this report. We study heavy quarkonium production at the Tevatron collider in the framework of the quasi-multi-Regge kinematics approach and the factorization formalism of nonrelativistic QCD at leading order in the strong-coupling constant α_s and the relative velocity v.

1 Introduction

Heavy quarkonium production at high energies has provided a useful laboratory for testing the high-energy limit of the quantum chromodynamics (QCD) as well as the interplay of perturbative and nonperturbative phenomena in the QCD. The factorization formalism of nonrelativistic QCD (NRQCD) [2] is a theoretical framework for the description of heavy-quarkonium production and decay. The factorization hypothesis of NRQCD assumes the separation of the effects of long and short distances in heavy quarkonium production. NRQCD is organized as a perturbative expansion in two small parameters, the strong-coupling constant α_s and the relative velocity v of the heavy quarks.

The phenomenology of strong interactions at high energies exhibits a dominant role of gluon interactions in quarkonium production. In the conventional parton model [3] (PM), the initial-state gluon dynamics is under the control of the Dokshitzer-Gribov-Lipatov-Altarelli-Parisi (DGLAP) evolution equation [4]. In this approach, it is assumed that $S > \mu^2 \gg \Lambda^2_{\rm QCD}$, where $\sqrt{S}$ is the invariant collision energy, μ is the typical energy scale of the hard interaction, and $\Lambda_{\rm QCD}$ is the asymptotic scale parameter. In this way, the DGLAP evolution equation takes into account only one big logarithm, namely $\ln(\mu/\Lambda_{QCD})$. In fact, the collinear approximation is used, and the transverse momenta of the initial gluons are neglected.

In the high-energy limit, the contribution from the partonic subprocesses involving t-channel gluon exchanges to the total cross section becomes dominant. The summation of the large logarithms $\ln(\sqrt{S}/\mu)$ in the evolution equation can then be more important than the one of the $\ln(\mu/\Lambda_{QCD})$ terms. In this case, the non-collinear gluon dynamics is described by the Balitsky-Fadin-Kuraev-Lipatov (BFKL) evolution equation [5]. In the region under consideration, the transverse momenta (k_T) of the incoming gluons and their off-shell properties can no longer be neglected, and we deal with *reggeized* t-channel gluons. The theoretical framework for this kind of high-energy phenomenology is the quasi-multi-Regge kinematics (QMRK) approach [6], which can be based on effective quantum field theory implemented with the non-abelian gauge-invariant action, as was suggested a few years ago [7].

Omitting the details of calculations, which were presented in our papers [1], we discuss here the obtained results on charmonium and bottomonium production at the Tevatron (run I and run II).

*e-mail: saleev@ssu.samara.ru
†e-mail: vasin@ssu.samara.ru

2 Charmonium production at the Tevatron

During the last decade, the CDF Collaboration at the Tevatron [8, 9] collected data on charmonium production at energies $\sqrt{S} = 1.8$ TeV (run I) and $\sqrt{S} = 1.96$ TeV (run II) in the central region of pseudorapidity $|\eta| < 0.6$. The data cover a large interval in transverse momentum, namely $5 < p_T < 20$ GeV (run I) and $0 < p_T < 20$ GeV (run II). The data sample of run I [8] includes p_T distributions of J/ψ mesons that were produced directly in the hard interaction, via radiative decays of χ_{cJ} mesons, via decays of ψ' mesons, and via decays of b hadrons. That of run II [9] includes p_T distributions of prompt J/ψ mesons, so far without separation into direct, χ_{cJ}-decay, and ψ'-decay contributions, and of J/ψ mesons from b-hadron decays.

In contrast to previous analyses we perform a joint fit to the run-I and run-II CDF data [8, 9] to obtain the color-octet non-perturbative matrix elements (NMEs) for J/ψ, ψ', and χ_{cJ} mesons. We use three different versions of unintegrated gluon distribution function. Our calculations are based on exact analytical expressions for the relevant squared amplitudes, which were previously unknown in literature. Our fits include five experimental data sets, which come as p_T distributions of J/ψ mesons from direct production, prompt production, χ_{cJ} decays, and ψ' decays in run I and from prompt production in run II.

In Table 1, we list out fit results for the relevant color-octet NMEs for three different choices of unintegrated gluon distribution function, namely JB [10], JS [11], and KMR [12]. The color-singlet NMEs are not fitted, but determined from the measured partial decay widths of $\psi(nS) \to l^+ + l^-$ and $\chi_{c2} \to \gamma + \gamma$. The numerical values are adopted from Ref. [13] and read: $\langle \mathcal{O}^{J/\psi}[^3S_1^{(1)}]\rangle = 1.3$ GeV^3, $\langle \mathcal{O}^{\psi'}[^3S_1^{(1)}]\rangle = 6.5 \times 10^{-1}$ GeV^3, and $\langle \mathcal{O}^{\chi_{cJ}}[^3P_J^{(1)}]\rangle = (2J+1) \times 8.9 \times 10^{-2}$ GeV^5. They were obtained using the vacuum saturation approximation and heavy-quark spin symmetry in the NRQCD factorization formulas and including next-to-leading order (NLO) QCD radiative corrections [14]. The relevant branching ratios are taken from Ref. [15] and read $B(J/\psi \to \mu^+ + \mu^-) = 0.0601$, $B(\psi' \to J/\psi + X) = 0.576$, $B(\chi_{c0} \to J/\psi + \gamma) = 0.012$, $B(\chi_{c1} \to J/\psi + \gamma) = 0.318$, and $B(\chi_{c2} \to J/\psi + \gamma) = 0.203$. They somewhat differ from the values used previously [16]. We take the pole mass of the chark quark to be $m_c = 1.55$ GeV. For comparison, we list in Table 1 also the NMEs obtained in Ref. [13] for the collinear PM with the leading order (LO) parton distribution functions of the proton by Martin, Roberts, Stirling, and Thorne (MRST98LO) [17].

We first study the relative importance of the different intermediate states in direct J/ψ and ψ' production. In previous fits to CDF data from run I [8], with $p_T > 5$ GeV, the linear combinations

$$M_r^{\mathcal{H}} = \langle \mathcal{O}^{\mathcal{H}}[^1S_0^{(8)}]\rangle + \frac{r}{m_c^2}\langle \mathcal{O}^{\mathcal{H}}[^3P_0^{(8)}]\rangle \tag{1}$$

for $\mathcal{H} = J/\psi, \psi'$ were fixed because it was infeasible to separate the contributions proportional to $\langle \mathcal{O}^{\mathcal{H}}[^1S_0^{(8)}]\rangle$ and $\langle \mathcal{O}^{\mathcal{H}}[^3P_0^{(8)}]\rangle$. By contrast, the new run II data [8], which reach down to $p_T = 0$, allow us to determine $\langle \mathcal{O}^{\mathcal{H}}[^1S_0^{(8)}]\rangle$ and $\langle \mathcal{O}^{\mathcal{H}}[^3P_0^{(8)}]\rangle$ separately because the respective contributions exhibit different p_T dependences for $p_T < 5$ GeV. We find that $\langle \mathcal{O}^{J/\psi,\psi'}[^3P_0^{(8)}]\rangle$ and $\langle \mathcal{O}^{\psi'}[^1S_0^{(8)}]\rangle$ are compatible with zero, independent of the choice of unintegrated gluon density. For the case of J/ψ production from ψ' decay, this implies that the $^3S_1^{(1)}$ and $^3S_1^{(8)}$ channels are sufficient to describe the measured p_T distribution (see Fig. 2).

In Figs. 1–4, we compare the CDF data on J/ψ mesons from direct production, ψ' decays, and χ_{cJ} decays in run I [8] and from prompt production in run II [9], respectively, with the theoretical results evaluated with the NMEs listed in Table 1. From Fig. 1, we observe that the color-singlet contribution is significant, especially at low values of p_T, and comparable to the one from the $^1S_0^{(8)}$ channel. As is familiar from the collinear PM, the $^3S_1^{(8)}$ contribution makes up the bulk of the cross section at large values of p_T. Incidentally, the values of $\langle \mathcal{O}^{J/\psi}[^3S_1^{(8)}]\rangle$ obtained in the QMRK framework are in average quite close to the one obtained in the collinear

PM, as may be seen from Table 1. The situation is very similar for J/ψ production from ψ' decay, considered in Fig. 2, except that the ${}^1S_0^{(8)}$ and ${}^3P_J^{(8)}$ contributions are negligible.

The discussion of J/ψ production from radiative χ_{cJ} decays, considered in Fig. 3, is simpler because there is only one free parameter in the fit, namely $\langle \mathcal{O}^{\chi_{c0}}[{}^3S_1^{(8)}]\rangle$. We confirm the conclusion of Ref. [18], that, in the QMRK approach, the color-singlet contribution is sufficient to describe the data. In fact, the best fit is realized when $\langle \mathcal{O}^{\chi_{c0}}[{}^3S_1^{(8)}]\rangle$ is taken to be zero or very small. In case of the JB gluon density, the fitting procedure even favors a negative value of $\langle \mathcal{O}^{\chi_{c0}}[{}^3S_1^{(8)}]\rangle$.

In Fig. 4, the p_T distribution of prompt J/ψ production in run II is broken down into the contributions from direct production, ψ' decays, and χ_{cJ} decays. We observe that the latter is dominant for $p_T > 5$ GeV, while prompt J/ψ mesons are preferably produced directly at larger values of p_T. The contribution from ψ' decays stays at the level of several percent for all values of p_T. While the JS [11] and KMR [12] gluon densities allow for a faithful description of the measured p_T distribution [9], the JB [10] one has a problem in the low-p_T range, at $p_T > 5$ GeV, where even the χ_{cJ}-decay contribution, which is entirely of color-singlet origin, exceeds the data. This problem can be traced to the speed of growth of the JB gluon density as $k_T \to 0$. By contrast, the JS and KMR gluon densities are smaller and approximately k_T independent at low values of k_T. For this reason, we excluded the CDF prompt-J/ψ data from run I [8] and run II [9] from our fit based on the JB gluon density.

Considering the color-octet NMEs relevant for the J/ψ, ψ' and χ_{cJ} production mechanisms, we can formulate the following heuristic rule for favored transitions from color-octet to color-singlet states: $\Delta L \simeq 0$ and $\Delta S \simeq 0$; *i.e.* these transitions are doubly chromoelectric and preserve the orbital angular momentum and the spin of the heavy-quark bound state.

3 Bottomonium production at the Tevatron

The CDF Collaboration at the Tevatron measured the p_T distributions of $\Upsilon(1S)$, $\Upsilon(2S)$, and $\Upsilon(3S)$ mesons in the central region of rapidity (y), $|y| < 0.4$, at $\sqrt{S} = 1.8$ TeV (run I) [19] and that of the $\Upsilon(1S)$ meson in the rapidity regions $|y| < 0.6$, $0.6 < |y| < 1.2$, and $1.2 < |y| < 1.8$ at $\sqrt{S} = 1.96$ TeV (run II) [20]. In both cases, the S-wave bottomonia were produced promptly, *i.e.*, directly or through non-forbidden decays of higher-lying S- and P-wave bottomonium states, including cascade transitions such as $\Upsilon(3S) \to \chi_{b1}(2P) \to \Upsilon(1S)$.

As is well known, the cross section of bottomonium production measured at the Tevatron at large values of p_T is more than one order of magnitude larger than the prediction of the color-singlet model (CSM) [21] implemented in the collinear PM [22]. Switching from the CSM to the NRQCD factorization formalism [2] within the collinear PM [23] somewhat ameliorates the situation in the large-p_T region, at $p_T \geq 10$ GeV, but still does not lead to agreement at all values of p_T. On the other hand, the shape of the p_T distribution can be described in the color evaporation model [24] improved by the resummation of the large logarithmic contributions from soft-gluon radiation at all orders in α_s in the region of $p_T < M$ [25], M is a heavy quarkonium mass. However, the overall normalization of the cross section can not be predicted in this approach [24, 25].

For the reader's convenience, we list in Table 2 the inclusive branching fractions of the feed-down decays of the various bottomonium states, which can be gleaned from Ref. [15]. Theses values superseed those presented in Ref. [23]. Since the $\Upsilon(nS)$ mesons are identified in Refs. [19, 20] through their decays to $\mu^+\mu^-$ pairs, we have to include the corresponding branching fractions, which we also adopt from Ref. [15], $B(\Upsilon(1S) \to \mu^+ + \mu^-) = 0.0248$, $B(\Upsilon(2S) \to \mu^+ + \mu^-) = 0.0131$, and $B(\Upsilon(3S) \to \mu^+ + \mu^-) = 0.0181$. We take the pole mass of the bottom quark to be $m_b = 4.77$ GeV.

In Table 3, we list out fit results for the relevant color-octet NMEs for three different choices

of unintegrated gluon distribution function, namely JB [10], KMR [12], and JS [11]. The relevant color-singlet NMEs are not fitted as the same as for charmonia. The partial decay widths of $\chi_{b0}(nP) \to 2\gamma$, from which the color-singlet NMEs of the $\chi_{bJ}(nP)$ mesons could be extracted, are yet unknown. However, these NMEs can be estimated using the wave functions evaluated at the origin from potential models [26], as was done in Ref. [23]. We adopt the color-singlet NMEs of the $\chi_{b0}(nP)$ mesons from Ref. [23].

In Figs. 5, 6, and 7, we compare the CDF data on prompt $\Upsilon(nS)$ hadroproduction in run I [19] with the theoretical results evaluated with the JB [10], JS [11], and KMR [12] unintegrated gluon distribution functions, respectively, and the NMEs listed in Table 3. In each case, the color-singlet and color-octet contributions are also shown separately. Except for the JB and KMR analyses of $\Upsilon(3S)$ production, the color-octet contributions are always suppressed, especially at low values of p_T. In the JS analysis, the $\Upsilon(1S)$ and $\Upsilon(2S)$ data are significantly exceeded by the color-singlet contributions for $p_T \leq 10$ GeV, which explains the poor quality of the fit, with $\chi^2/\text{d.o.f.} = 27$. In the JB analysis, this only happens for $p_T \leq 2$ GeV, so that the value of $\chi^2/\text{d.o.f.}$ is lowered by one order of magnitude, being $\chi^2/\text{d.o.f.} = 2.9$. By contrast, the KMR gluon yields an excellent fit, with $\chi^2/\text{d.o.f.} = 0.5$, and will be the only one considered in the following discussion. Comparing the color-singlet and color-octet contributions in Fig. 7, we observe that the latter is dominant in the $\Upsilon(3S)$ case and in the $\Upsilon(2S)$ case for $p_T \geq 13$ GeV, while it is of minor importance in the $\Upsilon(1S)$ case in the whole p_T range considered.

Notice that the contributions to prompt $\Upsilon(nS)$ hadroproduction due to the feed-down from the $\chi_{bJ}(3P)$ mesons have been neglected above, simply because the latter have not yet been observed and their partial decay widths are unknown. In the remainder of this section, we assess the impact of these contributions. For the color-singlet NME, we use the potential model result $\langle \mathcal{O}^{\chi_{b0}(3P)}[^3P_0^{(1)}]\rangle = 2.7$ GeV^5 [26]. By analogy to the KMR fit results for $\langle \mathcal{O}^{\chi_{b0}(1P)}[^3S_1^{(8)}]\rangle$ and $\langle \mathcal{O}^{\chi_{b0}(2P)}[^3S_1^{(8)}]\rangle$ in Table 3, we expect the value of $\langle \mathcal{O}^{\chi_{b0}(3P)}[^3S_1^{(8)}]\rangle$ to be negligibly small, compatible with zero. Looking at Table 2, a naive extrapolation from the $\chi_{bJ}(1P)$ and $\chi_{bJ}(2P)$ states suggests that the inclusive branching fractions for the $\chi_{bJ}(3P)$ decays into the $\Upsilon(3S)$, $\Upsilon(2S)$, and $\Upsilon(1S)$ states could be about 12%, 9%, and 7%, respectively. These decays generate further cascade transitions, whose inclusive branching fractions follow from these estimates in combination with the entries of Table 2. Including all these ingredients, we repeat our KMR fit to the CDF data. As illustrated in Fig. 8 for prompt $\Upsilon(nS)$ hadroproduction in run I, the CDF data can be fairly well described in the QMRK approach to the CSM, while the color-octet contributions turn out to be negligibly small. We note in passing that a similar observation, although with lower degree of agreement between data and theory, can be made for the JB gluon, while the JS gluon badly fails for $p_T \leq 10$ GeV.

4 Conclusion

Working at LO in the QMRK approach to NRQCD, we analytically evaluated the squared amplitudes of prompt heavy quarkonium production by *reggeized* gluons in $p\bar{p}$ collisions. We extracted the relevant color-octet NMEs, $\langle \mathcal{O}^{\mathcal{H}}[^{2S+1}L_J^{(8)}]\rangle$, for $\mathcal{H} = J/\psi$, χ_{cJ}, ψ', $\Upsilon(1S, 2S, 3S)$ and $\chi_{bJ}(1P, 2P)$ through fits to p_T distributions measured by the CDF Collaboration in $p\bar{p}$ collisions at the Tevatron with $\sqrt{S} = 1.8$ TeV [8, 19] and 1.96 TeV [9, 20] using three different unintegrated gluon distribution functions, namely JB [10], JS [11], and KMR [12]. The fits based on the KMR, JB, and JS gluons turned out to be excellent, fair, and poor, respectively.

The present analysis suggest that the color-octet NMEs of bottomonium are more strongly suppressed than those of charmonium as expected from the velocity scaling rules of NRQCD. We illustrated that the QMRK approach [6, 7] provides a useful laboratory to describe the phenomenology of high-energy processes in the Regge limit of QCD.

5 Acknowledgements

We would like to express our thanks to Prof. B. A. Kniehl with whom the results under discussion have been obtained. We thank Quarks'06 Organized Committee for the kind hospitality during the Conference. D.V. thanks the International Center of Fundamental Physics in Moscow and *Dynastiya* Foundation for the financial support received while this work was done.

References

[1] B. A. Kniehl, V. A. Saleev, and D. V. Vasin, Phys. Rev. D **73**, 074022 (2006); B. A. Kniehl, V. A. Saleev, and D. V. Vasin, Phys. Rev. D (to be published); V. A. Saleev, and D. V. Vasin, Vestnik SSU **40**, 126 (2005).

[2] G. T. Bodwin, E. Braaten, and G. P. Lepage, Phys. Rev. D **51**, 1125 (1995); **55**, 5853(E) (1997).

[3] CTEQ Collaboration, R. Brock *et al.*, Rev. Mod. Phys. **67**, 157 (1995).

[4] V. N. Gribov and L. N. Lipatov, Sov. J. Nucl. Phys. **15**, 438 (1972) [Yad. Fiz. **15**, 781 (1972)]; Yu. L. Dokshitzer, Sov. Phys. JETP **46**, 641 (1977) [Zh. Eksp. Teor. Fiz. **73**, 1216 (1977)]; G. Altarelli and G. Parisi, Nucl. Phys. **B126**, 298 (1977).

[5] E. A. Kuraev, L. N. Lipatov, and V. S. Fadin, Sov. Phys. JETP **44**, 443 (1976) [Zh. Eksp. Teor. Fiz. **71**, 840 (1976)]; I. I. Balitsky and L. N. Lipatov, Sov. J. Nucl. Phys. **28**, 822 (1978) [Yad. Fiz. **28**, 1597 (1978)].

[6] V. S. Fadin and L. N. Lipatov, Nucl. Phys. **B477**, 767 (1996); E. N. Antonov, L. N. Lipatov, E. A. Kuraev, and I. O. Cherednikov, Nucl. Phys. **B721**, 111 (2005).

[7] L. N. Lipatov, Nucl. Phys. **B452**, 369 (1995).

[8] CDF Collaboration, F. Abe *et al.*, Phys. Rev. Lett. **79**, 572 (1997); **79**, 578 (1997); CDF Collaboration, T. Affolder *et al.*, Phys. Rev. Lett. **85**, 2886 (2000).

[9] CDF Collaboration, D. Acosta *et al.*, Phys. Rev. D **71**, 032001 (2005).

[10] J. Blümlein, Report No. DESY 95-121 (1995).

[11] H. Jung and G. P. Salam, Eur. Phys. J. C **19**, 351 (2001).

[12] M. A. Kimber, A. D. Martin, and M. G. Ryskin, Phys. Rev. D **63**, 114027 (2001).

[13] E. Braaten, B. A. Kniehl, and J. Lee, Phys. Rev. D **62**, 094005 (2000).

[14] R. Barbieri, R. Gatto, R. Kögerler, and Z. Kunszt, Phys. Lett. B **57**, 455 (1975); R. Barbieri, M. Caffo, R. Gatto, and E. Remiddi, Nucl. Phys. **B192**, 61 (1981).

[15] Particle Data Group, S. Eidelman *et al.*, Phys. Lett. B **592**, 1 (2004).

[16] Particle Data Group, K. Hagiwara *et al.*, Phys. Rev. D **66**, 010001 (2002).

[17] A. D. Martin, R. G. Roberts, W. J. Stirling, and R. S. Thorne, Eur. Phys. J. C **4**, 463 (1998).

[18] Ph. Hägler, R. Kirschner, A. Schäfer, L. Szymanowski, and O. V. Teryaev, Phys. Rev. D **62**, 071502 (2000); Phys. Rev. Lett. **86**, 1446 (2001).

[19] CDF Collaboration, F. Abe *et al.*, Phys. Rev. Lett. **75**, 4358 (1995); CDF Collaboration, D. Acosta *et al.*, *ibid.* **88**, 161802 (2002).

[20] CDF Collaboration, V. M. Abazov *et al.*, Phys. Rev. Lett. **94**, 232001 (2005).

[21] V. G. Kartvelishvili, A. K. Likhoded, and S. R. Slabospitsky, Sov. J. Nucl. Phys. **28**, 678 (1978) [Yad. Fiz. **28**, 1315 (1978)]; E. L. Berger and D. Jones, Phys. Rev. D **23**, 1521 (1981); R. Baier and R. Rückl, Phys. Lett. B **102**, 364 (1981).

[22] N. Brambilla *et al.*, CERN Yellow Report No. FERMILAB-FN-0779, CERN-2005-005 (2005).

[23] E. Braaten, S. Fleming, and A. K. Leibovich, Phys. Rev. D **63**, 094006 (2001).

[24] J. F. Amundson, O. J. P. Eboli, E. M. Gregores, and F. Halzen, Phys. Lett. B **390**, 323 (1997).

[25] E. L. Berger, J. Qiu, and Y. Wang, Phys. Rev. D **71**, 034007 (2005); Int. J. Mod. Phys. A **20**, 3753 (2005).

[26] W. Lucha, F. F. Schoberl, and D. Gromes, Phys. Rept. **200**, 127 (1991); E. J. Eichten and C. Quigg, Phys. Rev. D **52**, 1726 (1995).

[27] CTEQ Collaboration, H. L. Lai *et al.*, Eur. Phys. J. C **12**, 375 (2000).

Table 1: NMEs for J/ψ, ψ', and χ_{cJ} mesons from fits in the collinear PM and in the QMRK approach using the JB [10], JS [11], and KMR [12] unintegrated gluon distribution functions. The CDF prompt data from run I [8] and run II [9] have been excluded from our fit based on the JB gluon density, if these data have been included the χ^2/d.o.f becomes greater then 20.

NME	PM [13]	Fit JB	Fit JS	Fit KMR
$\langle\mathcal{O}^{J/\psi}[^3S_1^{(1)}]\rangle/\mathrm{GeV}^3$	1.3±0.1	1.3±0.1	1.3±0.1	1.3±0.1
$\langle\mathcal{O}^{J/\psi}[^3S_1^{(8)}]\rangle/\mathrm{GeV}^3$	$(4.4\pm0.7)\times10^{-3}$	$(1.5\pm0.1)\times10^{-3}$	$(6.1\pm0.2)\times10^{-3}$	$(2.7\pm0.1)\times10^{-3}$
$\langle\mathcal{O}^{J/\psi}[^1S_0^{(8)}]\rangle/\mathrm{GeV}^3$	$\cdots$	$(6.6\pm2.3)\times10^{-3}$	$(9.0\pm0.6)\times10^{-3}$	$(1.4\pm0.1)\times10^{-2}$
$\langle\mathcal{O}^{J/\psi}[^3P_0^{(8)}]\rangle/\mathrm{GeV}^5$	$\cdots$	$(0.0\pm7.0)\times10^{-4}$	$(0.0\pm6.6)\times10^{-5}$	$(0.0\pm3.5)\times10^{-5}$
$M_{3.4}^{J/\psi}/\mathrm{GeV}^3$	$(8.7\pm0.9)\times10^{-2}$	$(6.6\pm3.3)\times10^{-3}$	$(9.0\pm0.7)\times10^{-3}$	$(1.4\pm0.1)\times10^{-2}$
$\langle\mathcal{O}^{\psi'}[^3S_1^{(1)}]\rangle/\mathrm{GeV}^3$	$(6.5\pm0.6)\times10^{-1}$	$(6.5\pm0.6)\times10^{-1}$	$(6.5\pm0.6)\times10^{-1}$	$(6.5\pm0.6)\times10^{-1}$
$\langle\mathcal{O}^{\psi'}[^3S_1^{(8)}]\rangle/\mathrm{GeV}^3$	$(4.2\pm0.1)\times10^{-3}$	$(3.0\pm0.5)\times10^{-4}$	$(1.5\pm0.2)\times10^{-3}$	$(8.3\pm0.9)\times10^{-4}$
$\langle\mathcal{O}^{\psi'}[^1S_0^{(8)}]\rangle/\mathrm{GeV}^3$	$\cdots$	$(0.0\pm3.5)\times10^{-4}$	$(0.0\pm3.9)\times10^{-4}$	$(0.0\pm5.8)\times10^{-4}$
$\langle\mathcal{O}^{\psi'}[^3P_0^{(8)}]\rangle/\mathrm{GeV}^5$	$\cdots$	$(0.0\pm1.0)\times10^{-4}$	$(0.0\pm7.1)\times10^{-5}$	$(0.0\pm5.3)\times10^{-5}$
$M_{3.5}^{\psi'}/\mathrm{GeV}^3$	$(1.3\pm0.5)\times10^{-2}$	$(0.0\pm4.9)\times10^{-4}$	$(0.0\pm4.9)\times10^{-5}$	$(0.0\pm6.5)\times10^{-4}$
$\langle\mathcal{O}^{\chi_{c0}}[^3P_0^{(1)}]\rangle/\mathrm{GeV}^5$	$(8.9\pm1.3)\times10^{-2}$	$(8.9\pm1.3)\times10^{-2}$	$(8.9\pm1.3)\times10^{-2}$	$(8.9\pm1.3)\times10^{-2}$
$\langle\mathcal{O}^{\chi_{c0}}[^3S_1^{(8)}]\rangle/\mathrm{GeV}^3$	$(2.3\pm0.3)\times10^{-3}$	$(0.0\pm4.0)\times10^{-6}$	$(2.2\pm0.9)\times10^{-4}$	$(4.7\pm4.7)\times10^{-5}$
χ^2/d.o.f.	$\cdots$	2.2	4.1	3.0

Table 2: Inclusive branching fractions of the feed-down decays of the various bottomonium states.

In\Out	$\Upsilon(3S)$	$\chi_{b2}(2P)$	$\chi_{b1}(2P)$	$\chi_{b0}(2P)$	$\Upsilon(2S)$	$\chi_{b2}(1P)$	$\chi_{b1}(1P)$	$\chi_{b0}(1P)$	$\Upsilon(1S)$
$\Upsilon(3S)$	1	0.114	0.113	0.054	0.106	0.007208	0.00742	0.004028	0.102171
$\chi_{b2}(2P)$	$\cdots$	1	$\cdots$	$\cdots$	0.162	0.011016	0.01134	0.006156	0.129565
$\chi_{b1}(2P)$	$\cdots$	$\cdots$	1	$\cdots$	0.21	0.01428	0.0147	0.00798	0.160917
$\chi_{b0}(2P)$	$\cdots$	$\cdots$	$\cdots$	1	0.046	0.003128	0.00322	0.001748	0.0167195
$\Upsilon(2S)$	$\cdots$	$\cdots$	$\cdots$	$\cdots$	1	0.068	0.07	0.038	0.319771
$\chi_{b2}(1P)$	$\cdots$	$\cdots$	$\cdots$	$\cdots$	$\cdots$	1	$\cdots$	$\cdots$	0.22
$\chi_{b1}(1P)$	$\cdots$	$\cdots$	$\cdots$	$\cdots$	$\cdots$	$\cdots$	1	$\cdots$	0.35
$\chi_{b0}(1P)$	$\cdots$	$\cdots$	$\cdots$	$\cdots$	$\cdots$	$\cdots$	$\cdots$	1	0.06
$\Upsilon(1S)$	$\cdots$	$\cdots$	$\cdots$	$\cdots$	$\cdots$	$\cdots$	$\cdots$	$\cdots$	1

Table 3: NMEs of the $\Upsilon(1S)$, $\Upsilon(2S)$, $\Upsilon(3S)$, $\chi_{b0}(1P)$, and $\chi_{b0}(2P)$ mesons from fits to CDF data from run I [19] and run II [20] in the collinear PM [23] using the CTEQ5L [27] parton distribution functions of the proton and in the QMRK approach using the JB [10], JS [11], and KMR [12] unintegrated gluon distribution functions of the proton. The errors on the fit results are determined by varying in turn each NME up and down about its central value until the value of χ^2 is increased by unity keeping all other NMEs fixed at their central values.

NME	PM [23]	Fit JB	Fit JS	Fit KMR
$\langle\mathcal{O}^{\Upsilon(1S)}[^3S_1^{(1)}]\rangle/\mathrm{GeV}^3$	10.9 ± 1.6	10.9 ± 1.6	10.9 ± 1.6	10.9 ± 1.6
$\langle\mathcal{O}^{\Upsilon(1S)}[^3S_1^{(8)}]\rangle/\mathrm{GeV}^3$	$\left(2.0\pm4.1^{-0.6}_{+0.5}\right)\times10^{-2}$	$(5.3\pm0.5)\times10^{-3}$	$(0.0\pm1.8)\times10^{-4}$	$(0.0\pm3.1)\times10^{-3}$
$\langle\mathcal{O}^{\Upsilon(1S)}[^1S_0^{(8)}]\rangle/\mathrm{GeV}^3$	$\cdots$	$(0.0\pm4.7)\times10^{-4}$	$(0.0\pm5.2)\times10^{-5}$	$(0.0\pm4.3)\times10^{-3}$
$\langle\mathcal{O}^{\Upsilon(1S)}[^3P_0^{(8)}]\rangle/\mathrm{GeV}^5$	$\cdots$	$(0.0\pm1.3)\times10^{-3}$	$(0.0\pm1.6)\times10^{-4}$	$(9.5\pm2.0)\times10^{-2}$
$M_5^{\Upsilon(1S)}/\mathrm{GeV}^3$	$\left(1.4\pm0.7^{+1.0}_{-0.7}\right)\times10^{-1}$	$(0.0\pm7.6)\times10^{-4}$	$(0.0\pm8.7)\times10^{-5}$	$(2.1\pm0.9)\times10^{-2}$
$\langle\mathcal{O}^{\chi_{b0}(1P)}[^3P_0^{(1)}]\rangle/\mathrm{GeV}^5$	2.4 ± 0.4	2.4 ± 0.4	2.4 ± 0.4	2.4 ± 0.4
$\langle\mathcal{O}^{\chi_{b0}(1P)}[^3S_1^{(8)}]\rangle/\mathrm{GeV}^3$	$\left(1.5\pm1.1^{+1.3}_{-1.0}\right)\times10^{-2}$	$(0.0\pm2.1)\times10^{-3}$	$(0.0\pm8.4)\times10^{-5}$	$(0.0\pm1.4)\times10^{-3}$
$\langle\mathcal{O}^{\Upsilon(2S)}[^3S_1^{(1)}]\rangle/\mathrm{GeV}^3$	4.5 ± 0.7	4.5 ± 0.7	4.5 ± 0.7	4.5 ± 0.7
$\langle\mathcal{O}^{\Upsilon(2S)}[^3S_1^{(8)}]\rangle/\mathrm{GeV}^3$	$\left(1.6\pm0.6^{+0.7}_{-0.5}\right)\times10^{-1}$	$(0.0\pm5.9)\times10^{-3}$	$(0.0\pm4.1)\times10^{-4}$	$(3.3\pm0.8)\times10^{-2}$
$\langle\mathcal{O}^{\Upsilon(2S)}[^1S_0^{(8)}]\rangle/\mathrm{GeV}^3$	$\cdots$	$(0.0\pm9.2)\times10^{-4}$	$(0.0\pm8.3)\times10^{-5}$	$(0.0\pm3.7)\times10^{-3}$
$\langle\mathcal{O}^{\Upsilon(2S)}[^3P_0^{(8)}]\rangle/\mathrm{GeV}^5$	$\cdots$	$(0.0\pm2.6)\times10^{-3}$	$(0.0\pm2.8)\times10^{-4}$	$(0.0\pm1.6)\times10^{-2}$
$M_5^{\Upsilon(2S)}/\mathrm{GeV}^3$	$\left(-1.1\pm1.0^{+0.3}_{-0.2}\right)\times10^{-1}$	$(0.0\pm1.5)\times10^{-3}$	$(0.0\pm1.4)\times10^{-4}$	$(0.0\pm7.2)\times10^{-3}$
$\langle\mathcal{O}^{\chi_{b0}(2P)}[^3P_0^{(1)}]\rangle/\mathrm{GeV}^5$	2.6 ± 0.5	2.6 ± 0.5	2.6 ± 0.5	2.6 ± 0.5
$\langle\mathcal{O}^{\chi_{b0}(2P)}[^3S_1^{(8)}]\rangle/\mathrm{GeV}^3$	$\left(0.8\pm1.1^{+1.1}_{-0.8}\right)\times10^{-2}$	$(1.1\pm0.4)\times10^{-2}$	$(0.0\pm2.8)\times10^{-4}$	$(0.0\pm5.7)\times10^{-3}$
$\langle\mathcal{O}^{\Upsilon(3S)}[^3S_1^{(1)}]\rangle/\mathrm{GeV}^3$	4.3 ± 0.9	4.3 ± 0.9	4.3 ± 0.9	4.3 ± 0.9
$\langle\mathcal{O}^{\Upsilon(3S)}[^3S_1^{(8)}]\rangle/\mathrm{GeV}^3$	$\left(3.6\pm1.9^{+1.8}_{-1.3}\right)\times10^{-2}$	$(1.4\pm0.3)\times10^{-2}$	$(5.9\pm4.2)\times10^{-3}$	$(1.1\pm0.4)\times10^{-2}$
$\langle\mathcal{O}^{\Upsilon(3S)}[^1S_0^{(8)}]\rangle/\mathrm{GeV}^3$	$\cdots$	$(0.0\pm2.6)\times10^{-3}$	$(0.0\pm8.1)\times10^{-4}$	$(0.0\pm2.7)\times10^{-3}$
$\langle\mathcal{O}^{\Upsilon(3S)}[^3P_0^{(8)}]\rangle/\mathrm{GeV}^5$	$\cdots$	$(2.4\pm0.8)\times10^{-2}$	$(3.4\pm4.2)\times10^{-3}$	$(5.2\pm1.1)\times10^{-2}$
$M_5^{\Upsilon(3S)}/\mathrm{GeV}^3$	$\left(5.4\pm4.3^{+3.1}_{-2.2}\right)\times10^{-2}$	$(5.2\pm4.4)\times10^{-3}$	$(7.4\pm10.2)\times10^{-4}$	$(1.1\pm0.5)\times10^{-2}$
$\langle\mathcal{O}^{\chi_{b0}(3P)}[^3P_0^{(1)}]\rangle/\mathrm{GeV}^5$	2.7 ± 0.7	2.7 ± 0.7	2.7 ± 0.7	2.7 ± 0.7
χ^2/d.o.f.	$\cdots$	2.9	27	0.5

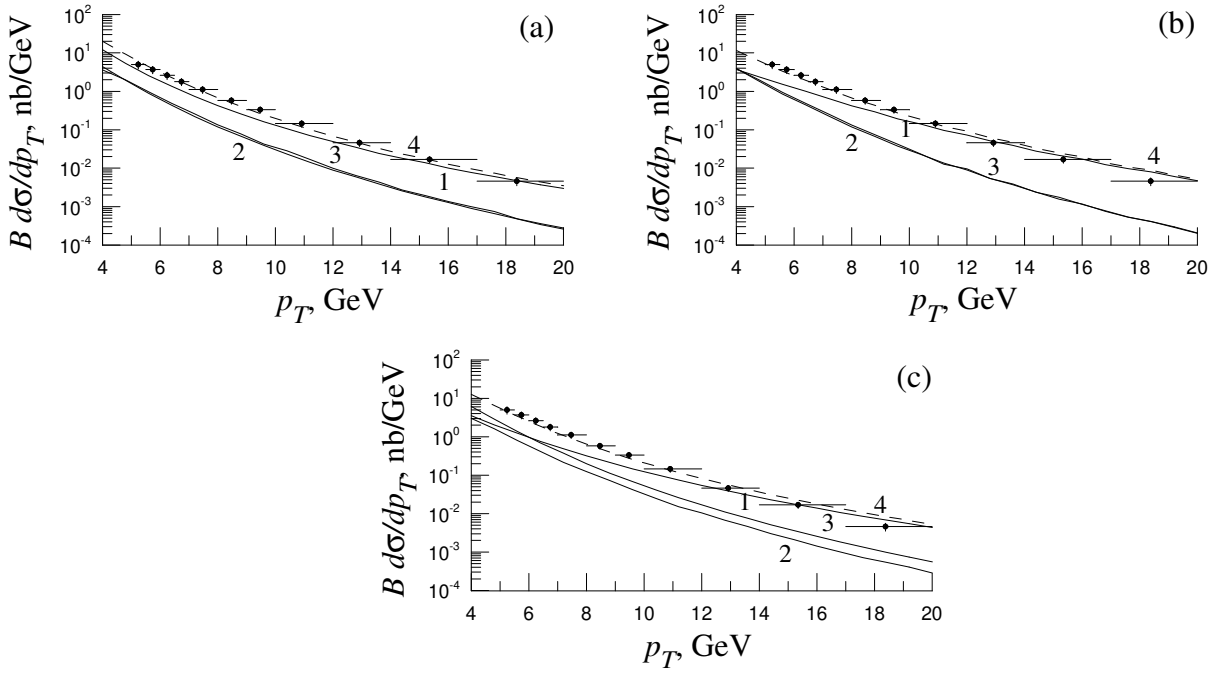

Figure 1: Contributions to the p_T distribution of direct J/ψ hadroproduction in $p\overline{p}$ scattering with $\sqrt{S} = 1.8$ TeV and $|y| < 0.6$ from the partonic subprocesses (1) $R + R \to J/\psi[^3S_1^{(8)}]$, (2) $R + R \to J/\psi[^1S_0^{(8)}, ^3P_J^{(8)}]$, (3) $R + R \to J/\psi[^3S_1^{(1)}] + g$, and (4) their sum compared with CDF data from Tevatron run I [8]. The theoretical results are obtained with the (a) JB [10], (b) JS [11], or (c) KMR [12] unintegrated gluon distribution functions. The decay branching fraction $B(J/\psi \to \mu^+ + \mu^-)$ is included.

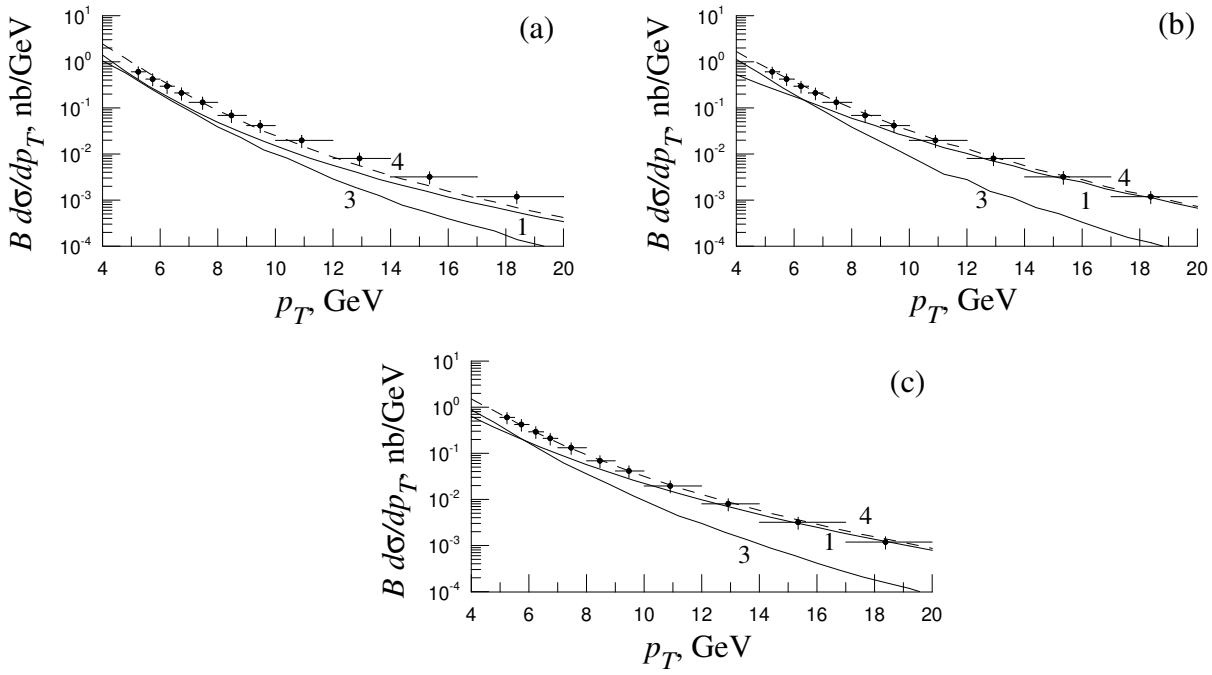

Figure 2: Contributions to the p_T distribution of J/ψ mesons from ψ' decays in hadroproduction in $p\overline{p}$ scattering with $\sqrt{S} = 1.8$ TeV and $|y| < 0.6$ from the partonic subprocesses (1) $R + R \to \psi'[^3S_1^{(8)}]$, (2) $R + R \to \psi'[^1S_0^{(8)}, ^3P_J^{(8)}]$ (this contribution actually vanished), (3) $R + R \to \psi'[^3S_1^{(1)}] + g$, and (4) their sum compared with CDF data from Tevatron run I [8]. The theoretical results are obtained with the (a) JB [10], (b) JS [11], or (c) KMR [12] unintegrated gluon distribution functions. The decay branching fraction $B(J/\psi \to \mu^+ + \mu^-)$ is included.

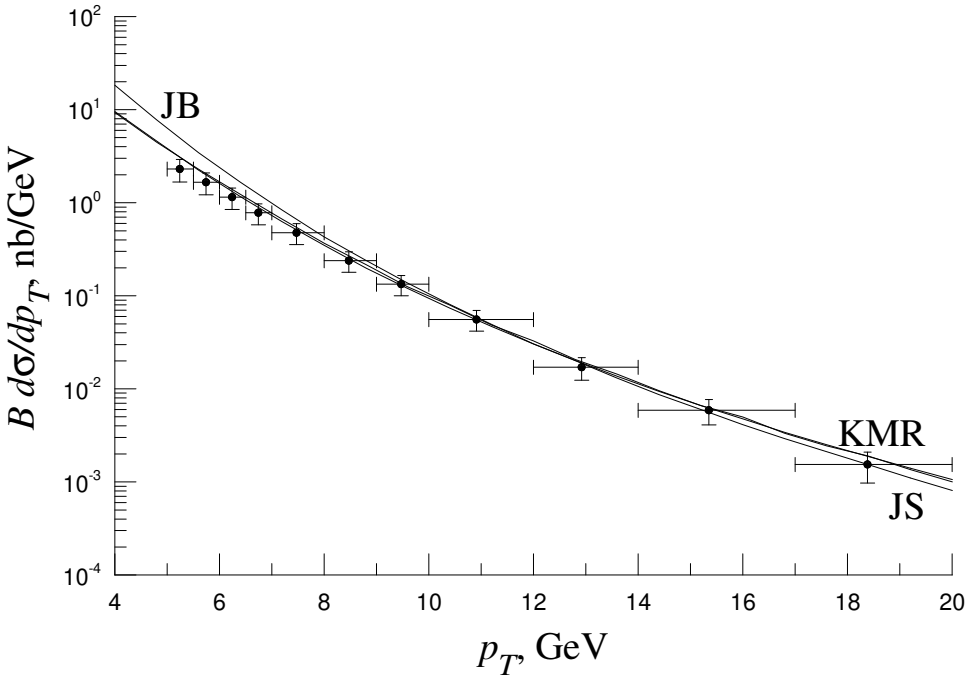

Figure 3: Contributions to the p_T distribution of J/ψ mesons from χ_{cJ} decays in hadroproduction in $p\overline{p}$ scattering with $\sqrt{S} = 1.8$ TeV and $|y| < 0.6$ from the sum of the partonic subprocesses $R + R \to \chi_{cJ}[^3P_J^{(1)}]$ and $R + R \to \chi_{cJ}[^3S_1^{(8)}]$, the latter of which being quite unimportant, compared with CDF data from Tevatron run I [8]. The theoretical results are obtained with the JB [10], JS [11], or KMR [12] unintegrated gluon distribution functions. The decay branching fraction $B(J/\psi \to \mu^+ + \mu^-)$ is included.

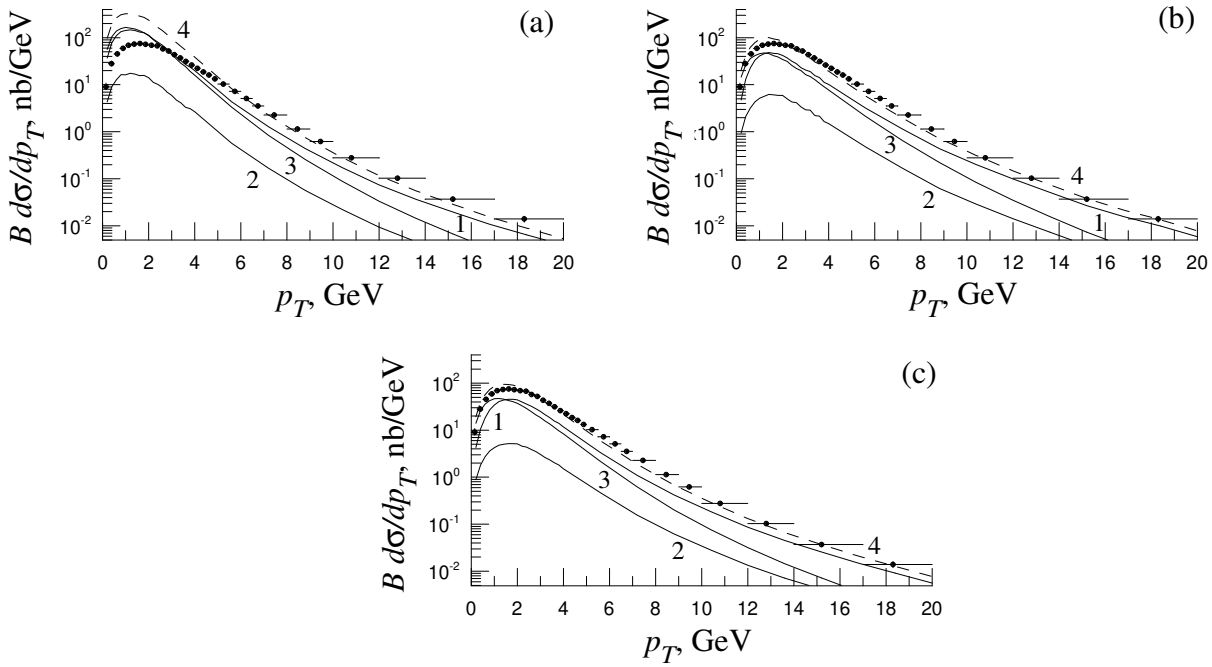

Figure 4: Contributions to the p_T distribution of prompt J/ψ hadroproduction in $p\overline{p}$ scattering with $\sqrt{S} = 1.96$ TeV and $|y| < 0.6$ from (1) direct production, (2) ψ' decays, (3) χ_{cJ} decays, and (4) their sum compared with CDF data from Tevatron run II [9]. The theoretical results are obtained with the (a) JB [10], (b) JS [11], or (c) KMR [12] unintegrated gluon distribution functions. The decay branching fraction $B(J/\psi \to \mu^+ + \mu^-)$ is included.

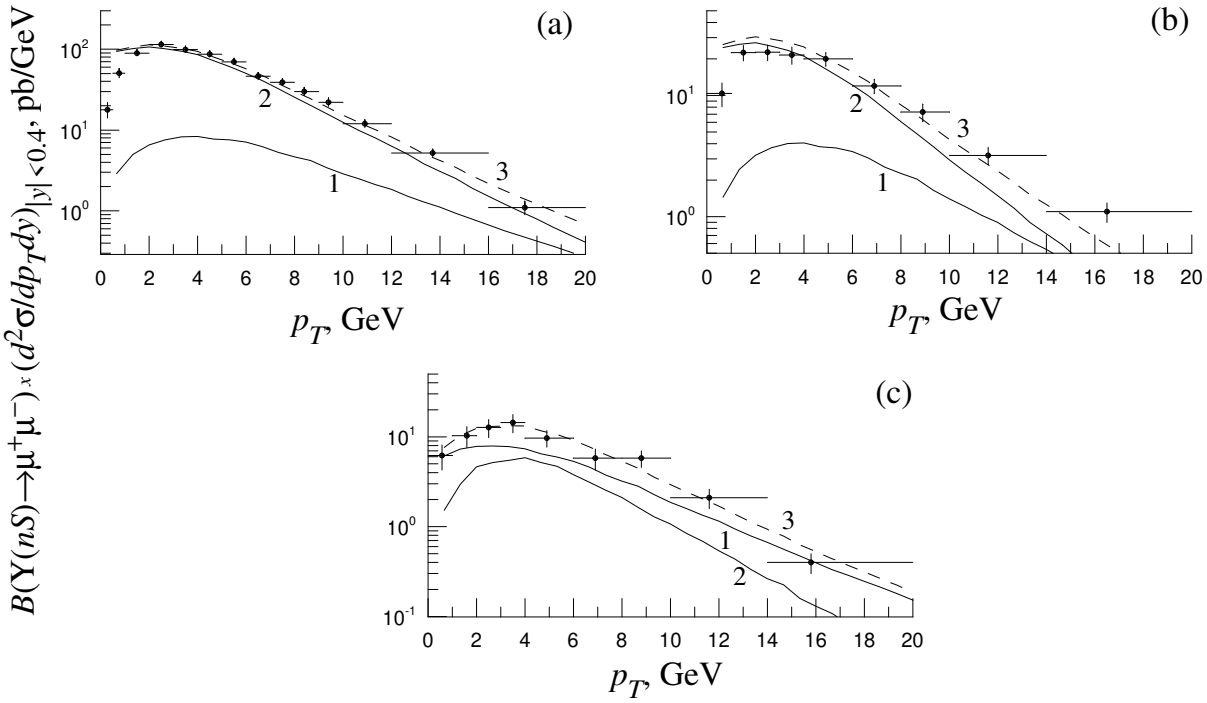

Figure 5: p_T distributions of prompt (a) $\Upsilon(1S)$, (b) $\Upsilon(2S)$, and (c) $\Upsilon(3S)$ hadroproduction in $p\overline{p}$ scattering with $\sqrt{S} = 1.8$ TeV and $|y| < 0.4$ including the respective decay branching fractions $B(\Upsilon(nS) \to \mu^+ + \mu^-)$. The color-octet (curve 1) and color-singlet (curve 2) contributions, evaluated with the JB [10] unintegrated gluon distribution function, and their sum (curve 3) are compared with the CDF data from run I [19].

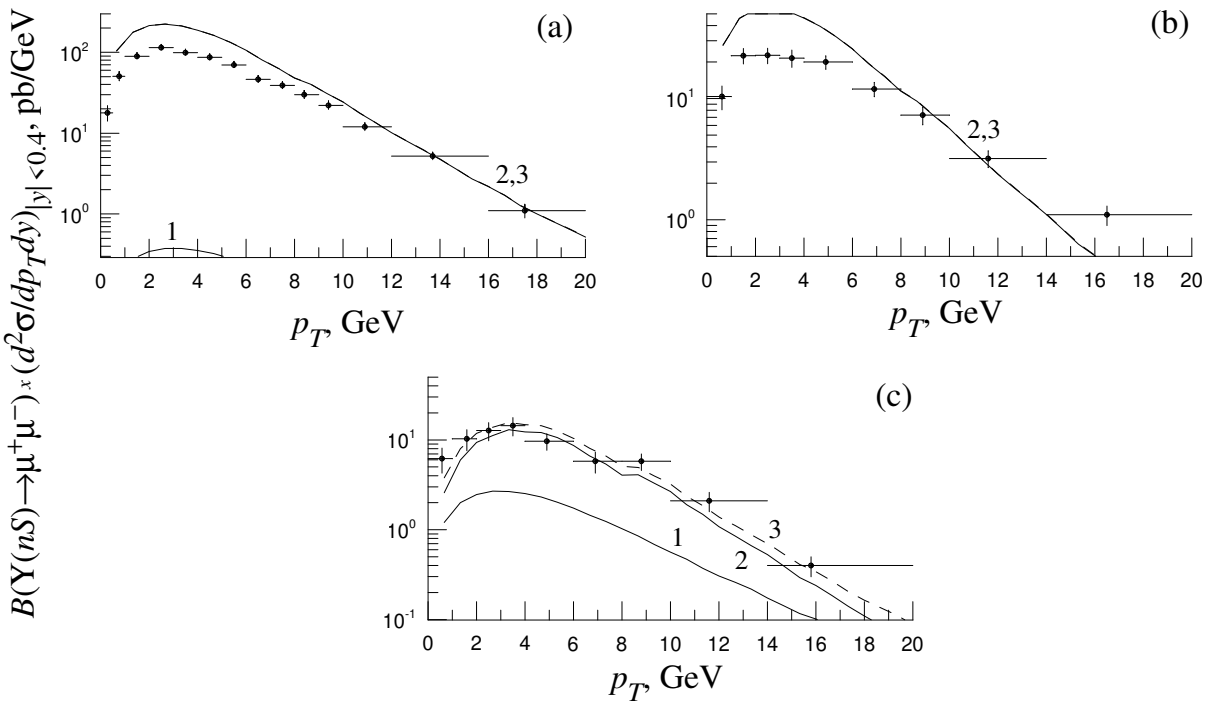

Figure 6: Same as in Fig. 5, but for the JS [11] unintegrated gluon distribution function.

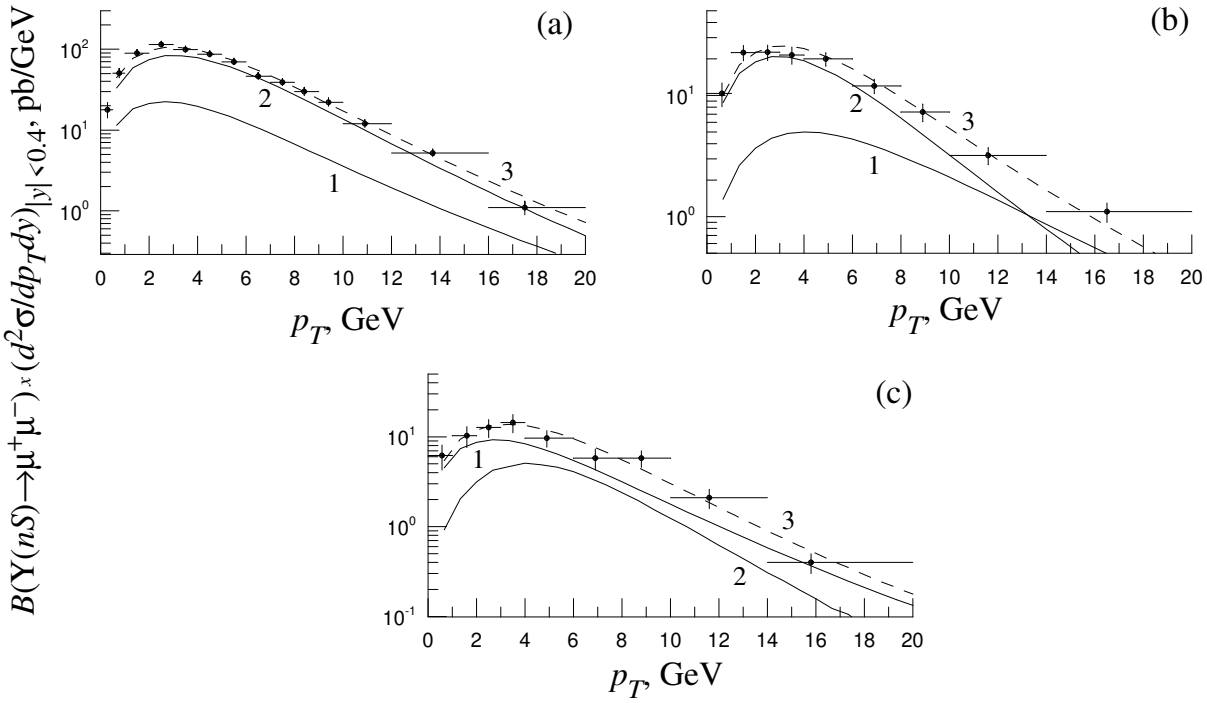

Figure 7: Same as in Fig. 5, but for the KMR [12] unintegrated gluon distribution function.

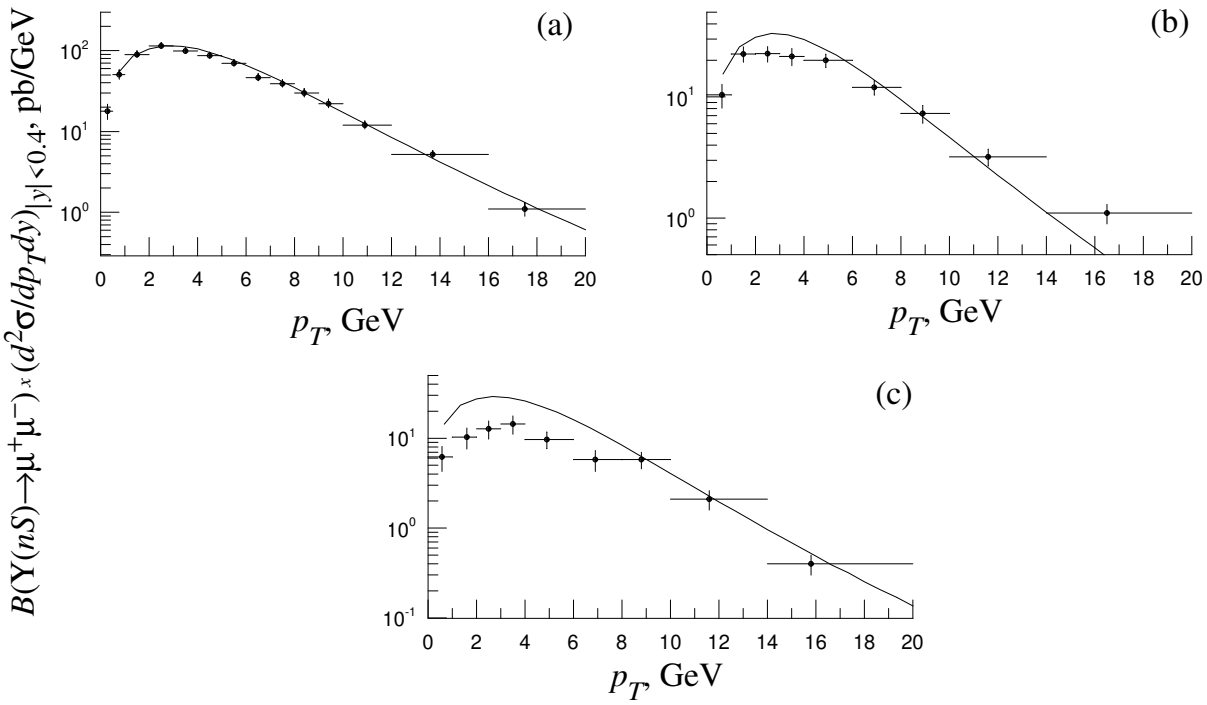

Figure 8: p_T distributions of prompt (a) $\Upsilon(1S)$, (b) $\Upsilon(2S)$, and (c) $\Upsilon(3S)$ hadroproduction in $p\overline{p}$ scattering with $\sqrt{S} = 1.8$ TeV and $|y| < 0.4$ including the respective decay branching fractions $B(\Upsilon(nS) \to \mu^+ + \mu^-)$. The color-singlet contribution including the estimated feed-down contributions due to the $\chi_{bJ}(3P)$ meson, evaluated with the KMR [12] unintegrated gluon distribution function, is compared with the CDF data from run I [19].